

# We are IntechOpen, the world's leading publisher of Open Access books Built by scientists, for scientists

6,900

Open access books available

186,000

International authors and editors

200M

Downloads

Our authors are among the

154

Countries delivered to

TOP 1%

most cited scientists

12.2%

Contributors from top 500 universities



WEB OF SCIENCE™

Selection of our books indexed in the Book Citation Index  
in Web of Science™ Core Collection (BKCI)

Interested in publishing with us?  
Contact [book.department@intechopen.com](mailto:book.department@intechopen.com)

Numbers displayed above are based on latest data collected.  
For more information visit [www.intechopen.com](http://www.intechopen.com)



# The Role of Hydraulic Conductivity in Modeling the Movement of Water and Solutes in Soil Under Drip Irrigation

René Chipana Rivera  
*University Mayor de San Andrés*  
*La Paz*  
*Bolivia*

## 1. Introduction

Due of de need to manage more rational irrigation water in the world drip irrigation is one of the technologies that are expanding more rapidly in modern irrigated agriculture in view of its great potential to improve the economics of water use. In this method the water is provided in soil in a timely high frequency, and thus the dimension parameters such as percentage of the root zone moist, spacing and location of emitters, application rates, frequency and irrigation, are governed by standard distribution of moisture in the soil profile, which in turn depends on soil hydraulic conductivity. There is difficulty in pinpointing the relationships between factors that affect the movement of soil water in response to surface point sources, this fact is due to the complex nature of the surface boundary conditions, which can result in problems of irrigation management. Due to these facts, mathematical models were developed to analyze three-dimensional movement of water in soil under drip irrigation, using methods of numerical analysis, finite elements, flow in two and three dimensions under dynamic equilibrium, volume control, theory of capillary tubes, among others.

Moreover, in recent years, the technique of application of chemicals through irrigation water (chemigation) is gaining acceptance, particularly in drip irrigation systems, due to the advantages it provides the possibility of manipulating and controlling plant nutrition irrigated. However, this technique requires that the irrigation is carried out under high efficiencies, otherwise it may cause economic problems and environmental damage. The chemicals applied through irrigation water processes suffer from spatial and temporal changes in soil, varying the distribution of solutes in the profile, resulting in different distribution patterns. Some solutes react with the soil matrix, others move through it, may result in dissolution and precipitation, within or outside the soil solution. The understanding of the simultaneous transport of water and solutes in two or three dimensions, from a point source, allows to develop efficient strategies in the implementation of water and mineral fertilizers (fertigation). Although fertigation has widespread use, little information related to the simultaneous movement of water and chemicals from point sources is available.

The high costs involved in field research are making mathematical models a very viable tool, enabling a prediction and assessment of the fate and behavior of water and solutes in drip irrigation. However, the development of mathematical models to accurately describe the transport of water and solutes under real field conditions presents great complexity due to the large number of intervening factors, as well as the variability of hydraulic conductivity.

The hydraulic conductivity expressed the "ease" with which certain fluid flows in a way, dependent on the medium and fluid. The main characteristics of the soil matrix that interfere with the hydraulic conductivity are the distribution of the diameters of the pores, the tortuosity, specific surface area and porosity. In the fluid, the main features are the density and dynamic viscosity. The methods for determining the hydraulic conductivity can be classified into permanent, variable and computing. The direct measurement of hydraulic conductivity is theoretically simple, but experimentally difficult, because of their high variability in the field.

## 2. Model water and solute movement

The modeling was based on the numerical solution of two partial differential equations of second order applied to point sources under transient flow, ie the equation of motion of water in the soil also known as the Richards equation (equation 1) and the transport equation solutes (equation 2, considering the existence of linear equilibrium sorption), allowing to determine the distribution of water and solutes in soil as a function of both space and time

$$\frac{\partial \theta}{\partial t} = \frac{\partial}{\partial x} \left[ K_x(\theta) \frac{\partial H}{\partial x} \right] + \frac{\partial}{\partial y} \left[ K_y(\theta) \frac{\partial H}{\partial y} \right] + \frac{\partial}{\partial z} \left[ K_z(\theta) \frac{\partial H}{\partial z} \right] \quad (1)$$

where  $\theta$  is the soil moisture ( $L^3 L^{-3}$ ),  $t$  time (T),  $K(\theta)$  is the hydraulic conductivity of unsaturated soil ( $L T^{-1}$ ),  $H$  is the total hydraulic potential of water in the soil (L),  $x$ ,  $y$  and  $z$  position coordinates

$$Fr \frac{\partial \theta C}{\partial t} = - \frac{\partial(qC)}{\partial z} + \frac{\partial}{\partial z} \left[ D\theta \frac{\partial C}{\partial z} \right] - \frac{\partial(qC)}{\partial x} + \frac{\partial}{\partial x} \left[ D\theta \frac{\partial C}{\partial x} \right] - \frac{\partial(qC)}{\partial y} + \frac{\partial}{\partial y} \left[ D\theta \frac{\partial C}{\partial y} \right] \quad (2)$$

Where  $C$  is the mass of solute per unit volume of solution ( $M L^{-3}$ ),  $q$  the volume of liquid (solution) through unit area of soil in unit time, also known as flux density ( $LT^{-1}$ ),  $D$  is the diffusion coefficient of dispersion, also known as hydrodynamic dispersion coefficient,  $Fr$  is the retardation factor, dimensionless, defined by:

$$Fr = 1 + \frac{\rho K_d}{\theta} \quad (3)$$

where  $\rho$  is the density of the soil ( $M L^{-3}$ ),  $K_d$  distribution coefficient or partition ( $L^3 M^{-1}$ ).

The retardation factor can be defined as the ability to retain or effect "buffer" of a particular element, or as the velocity of the solute in the speed of solution in the pore (Matos et al., 1999). If there are no interactions between the solute and soil, the  $K_d$  value is zero and the retardation factor becomes unity. If  $Fr$  is less than one means that only a fraction of the liquid phase participates in the transport process, as occurs for example in dense clusters

containing very small pore diameter (Van Genuchten & Wierenga, 1986). According Toride et al. (1999) there is a negative correlation between speed of solution in the pore ( $\vartheta$ , with dimensions  $LT^{-1}$ ) and distribution coefficient or partition ( $K_d$ ), implying that  $Fr$  and  $\vartheta$  are also inversely correlated.

Thus, the parameters of the soil dispersivity ( $\lambda$ , with dimensions  $L$ ) and  $Fr$ , determine the way forward or a solute is retained in the soil (Alvarez et al., 1995). The most direct way to determine the parameters  $\lambda$  and  $Fr$  is from experiments using soil columns, in which a solution is applied on top of the column and the values of solute concentration are collected in the output. Nielsen & Biggar (1962) indicate that the standard form of presentation of the concentration data collected at the exit is called the breakthrough curve, and one should be careful about using the correct boundary conditions, otherwise its use can lead to serious errors when experimental data are extrapolated to the field.

These equations were solved considering a system of control volumes, two-dimensionally characterized by radial and vertical dimensions ( $\Delta r$  and  $\Delta z$ , respectively) and performing successive increments of time ( $\Delta t$ ). In developing the model, we took into account the basic assumptions described by Botrel (1988) and Cruz (2000), under which the study region (wet bulb) can be described in a cylindrical space and imaginatively composed of rings concentric, each with a width ( $\Delta r$ ) and depth ( $\Delta z$ ). The rings have a center vertical line as part of that point source at the soil surface and vary in size according to their position ( $i$ ) and ( $j$ ), where ( $i$ ) represents the radial axis and ( $j$ ) axis vertical, as shown in figure 1.

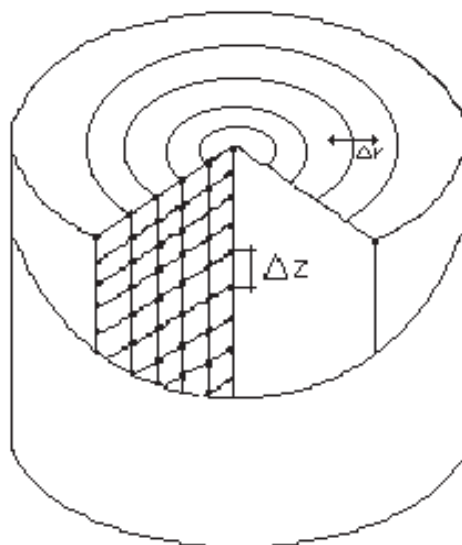


Fig. 1. Diagram of concentric rings considered for the numerical solution of the problem.

## 2.1 Determination of hydraulic conductivity and matric potential

The determination of hydraulic conductivity for unsaturated soils  $K(\theta)$  is initially carried out considering values of relative hydraulic conductivity ( $K_r$ , with dimensions  $L T^{-1}$ ) for conditions of no saturation calculated as a function of time and space.

Mualem (1976) and van Genuchten (1980) developed equations and methodologies for determining the hydraulic conductivity for unsaturated soils, from the relative hydraulic conductivity ( $K_r$ ), using parameters of water retention of soil water, as shown in equations 4 to 7.

$$\Theta = \frac{\theta - \theta_r}{\theta_s - \theta_r} \quad (4)$$

Where  $\Theta$  is the effective saturation, so reflecting on the water content in soil (dimensionless),  $\theta$  is the volumetric soil water content in the current condition ( $L^3 L^{-3}$ ),  $\theta_r$  is the residual soil water content ( $L^3 L^{-3}$ ),  $\theta_s$  is the volumetric soil water content at saturation point ( $L^3 L^{-3}$ ).

$\Theta$  can also be expressed by the equation 5:

$$\Theta = \left[ \frac{1}{1 + (\alpha\psi)^n} \right]^m \quad (5)$$

where  $m$  and  $n$  are regression parameters of equation (dimensionless),  $\alpha$  is the parameter with dimension equal to the reversal potential ( $L^{-1}$ ),  $\psi$  is the matrix water potential in soil ( $L$ ). Equation 6 expresses the value of relative hydraulic conductivity:

$$Kr = \Theta^{1/2} \left[ \frac{\int_0^\Theta \frac{1}{\psi(x)} dx}{\int_0^1 \frac{1}{\psi(x)} dx} \right]^2 \quad (6)$$

known value of  $Kr$  can be determined the value of hydraulic conductivity of unsaturated soil ( $K(\theta)$ ) as the product of relative hydraulic conductivity on the conductivity of saturated soil ( $K_o$ , with dimensions  $L T^{-1}$ ):

$$K(\theta) = Kr K_o \quad (7)$$

$Kr$  can also be calculated using equation (8), which is a consequence of equations (4, 5 and 6):

$$Kr = \Theta^{0,5} \left[ 1 - (1 - \Theta^{1/m})^m \right]^2 \quad (8)$$

On the other hand the matrix potential of soil water ( $\psi$ ) was determined by transforming the equation (5), as presented in equation (9):

$$\psi = \frac{\left[ \frac{1}{\Theta^{1/m}} - 1 \right]^2}{\alpha} \quad (9)$$

## 2.2 Transport of water in the soil profile

### 2.2.1 Calculating the volume of soil

When considering the soil divided into concentric rings, the axis of symmetry is formed by the vertical line passing through the wmitter. In this case, the first ring has a radius equal to half the increase in the horizontal axis ( $\Delta r/2$ ).

The calculation of the volume of soil was done by considering the volumes of the rings in the radial and vertical axes. For example, the volume of the ring ( $i, j$ ) is the volume of the cylinder defined by the larger radius of the ring ( $R_{ij}$ ), less the volume of the cylinder defined by the smaller radius of the ring ( $R_{i,j-1}$ ), considering a high  $\Delta z$ , as shown in equation (10).

$$V_{s(i,j)} = \pi(R_{i,j}^2 - R_{i,j-1}^2)\Delta z$$

(10)

where  $V_s$  is the volume of soil in each ring,  $L^3$ ,  $R$  is the radius of the ring,  $L$  and  $\Delta z$  is the depth of the ring,  $L$ . In vertical direction the volumes of the rings vary in function of their distance from the axis, but are constant for each position ( $j$ ), whatever the depth. The volume of water stored in each ring ( $V_a$ ) is determined by multiplying the volume of soil by the value of volumetric soil water content ( $\theta$ ):

$$V_a = V_s \theta$$

(11)

this calculation was performed for each time increment ( $\Delta T$ ) either in the radial direction and vertical

2.2.2 Determination of flux density (q)

The calculation of flux density ( $q$ ) from one cell to another was made following considerations advocated by van der Ploeg and Benecke (1974) and van Genuchten (1980), whereby it is assumed that the flow inside the rings or cells occurs in two directions, both for entry and exit for water and solutes (figure 2).

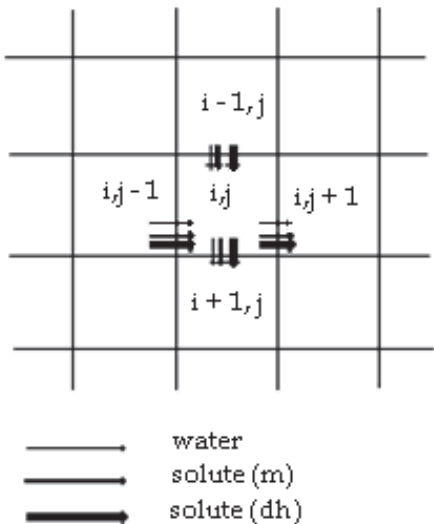


Fig. 2. Coordinates of adjacent cells required to determine the movement of water and solutes by convection (m) and hydrodynamic dispersion (dh) in the radial and vertical direction

a)Radial flux density

The movement of water from one ring to another in the radial axis is calculated according to equation (12).

$$q = -K(\theta)\frac{dH}{ds}$$

(12)

Considering that the flow occurs between two adjacent rings, it was assumed that the unsaturated hydraulic conductivity of the region where the flow takes place, can be represented by the unsaturated hydraulic conductivity of the medium adjacent rings.

$$K_{(i,j-1; i,j)} = \frac{K_{(i,j-1)} + K_{(i,j)}}{2} \quad (13)$$

where  $K_{(i,j-1; i,j)}$  is the average unsaturated hydraulic conductivity cell (i, j-1) and (i, j);  $K_{(i,j-1)}$  is the unsaturated conductivity cell (i, j-1) and  $K_{(i,j)}$  is the unsaturated hydraulic conductivity of the cell (i,j). Therefore the equation (12) for determining the water flow rewritten as can be follows:

$$q_{(i,j-1; i,j)} = -K_{(i,j-1; i,j)} \frac{H_{(i,j)} - H_{(i,j-1)}}{\Delta r} \quad (14)$$

where  $q_{(i,j-1; i,j)}$  is the flux density between the cell (i, j-1) and cell (i, j);  $H_{i,j}$  is the total hydraulic potential of water in cell (i, j);  $H_{i,j-1}$  is the total hydraulic potential of water in cell (i, j-1), and  $\Delta r$  is the increment in radius, ie the difference between the average radius of two cells.

Likewise, the radial flux density between the cell (i, j) and cell (i, j +1) is calculated on the basis of equations (15) and (16):

$$K_{(i,j; i,j+1)} = \frac{K_{(i,j)} + K_{(i,j+1)}}{2} \quad (15)$$

$$q_{(i,j; i,j+1)} = -K_{(i,j; i,j+1)} \frac{H_{(i,j+1)} - H_{(i,j)}}{\Delta r} \quad (16)$$

#### b) Vertical flux density

Similarly to the case of radial transport, the vertical flux density of cells (i-1, j) (i, j) and (i, j) (i +1, j), was determined by the following equations:

$$K_{(i-1,j; i,j)} = \frac{K_{(i-1,j)} + K_{(i,j)}}{2} \quad (17)$$

$$q_{(i-1,j; i,j)} = -K_{(i-1,j; i,j)} \frac{H_{(i,j)} - H_{(i-1,j)}}{\Delta z} \quad (18)$$

$$K_{(i,j; i+1,j)} = \frac{K_{(i,j)} + K_{(i+1,j)}}{2} \quad (19)$$

$$q_{(i,j; i+1,j)} = -K_{(i,j; i+1,j)} \frac{H_{(i+1,j)} - H_{(i,j)}}{\Delta z} \quad (20)$$

### 2.2.3 Moisture balance in each ring

Before and after application of water by a point source estimated the moisture at depth (i) and radial position (j) for each increment of time ( $\Delta t$ ). The volume of water flowing horizontally from cell (i, j-1) (i, j) is determined from the lateral area of each ring and the flux density:



$$Va_{(i,j-1;i,j)} = q_{(i,j-1;i,j)} 2\pi(R_{(i,j-1)}) \Delta z \Delta t \quad (21)$$

however the volume passing through the cell (i, j) (i, j + 1) is represented by:

$$Va_{(i,j;i,j+1)} = q_{(i,j;i,j+1)} 2\pi(R_{(i,j)}) \Delta z \Delta t \quad (22)$$

Similarly, the amount the volume of water flowing vertically between the rings (i-1, j) to (i, j) and (i, j) to (i + 1, j) is calculated by:

$$Va_{(i-1,j;i,j)} = q_{(i-1,j;i,j)} \pi(R_{(i,j)}^2 - R_{(i,j-1)}^2) \Delta t \quad (23)$$

$$Va_{(i,j;i+1,j)} = q_{(i,j;i+1,j)} \pi(R_{(i,j)}^2 - R_{(i,j-1)}^2) \Delta t \quad (24)$$

The amount of water that remained in a particular ring after the increment  $\Delta t$  is represented by the change in volume of water in the ring ( $\Delta Va_{(i,j)}$ ) due to water gain ( $Va_{(i,j-1 \text{ a } i,j)}$  and  $Va_{(i-1,j \text{ a } i,j)}$ ) and loss ( $Va_{(i,j \text{ a } i,j+1)}$  e  $Va_{(i,j \text{ a } i+1,j)}$ ), so:

$$\Delta Va_{(i,j)} = Va_{(i,j-1;i,j)} + Va_{(i-1,j;i,j)} - Va_{(i,j;i,j+1)} - Va_{(i,j;i+1,j)} \quad (25)$$

Thus, the new moisture ring at the end of  $\Delta t$  is calculated by equation (26):

$$\theta_{(i,j)} = \theta_{(i,j,ini)} + \frac{\Delta Va_{(i,j)}}{Vs_{(i,j)}} \quad (26)$$

where  $\theta_{(i,j,ini)}$  is the soil moisture at the beginning of the interval  $\Delta t$ ,  $L^3L^{-3}$ .

Therefore, when considering the control volume discretization, equation (1) to two dimensions is transformed into:

$$\frac{\Delta \theta}{\Delta t} = \frac{\Delta q_x}{\Delta x} + \frac{\Delta q_z}{\Delta z} \quad (27)$$

or

$$\frac{\Delta \theta}{\Delta t} = -\bar{K}_x(\theta) \frac{\Delta H_x}{\Delta x} - \bar{K}_z(\theta) \frac{\Delta H_z}{\Delta z} \quad (28)$$

One important hypothesis was considered for resolving cases in which the humidity inside the ring became greater than the moisture content under saturation ( $\theta_{(i,j)} > \theta_{s(i,j)}$ ). In this case the rings are the volume of surface water did not infiltrate transfer the water at outer rings (forming a circle saturated surface) and in the rings of the surface, the volume of water that can not be transported is held in the upper rings.

### 2.3 Solute transport in the bulb

After calculating the values of the volume of water flow and changes in moisture rings, starts determining the concentration of solute in each ring. Again the technique is employed to control volumes to calculate the mass flow, the flow by hydrodynamic dispersion and the variation of solute concentration in soil ( $\Delta C$ ).



### 2.3.1 Mass flow of solute

The mass flow of solute is determined for both the radial direction and for the vertical direction.

Radial mass flow

$$J_{c(i,j-1; i,j)} = q_{(i,j-1; i,j)} C_{(i,j-1)} \quad (29)$$

where  $J_{c(i,j-1; i,j)}$  is the mass flow of the solute in cell (i,j-1) to cell (i,j),  $ML^{-2}T^{-1}$ .

$$J_{c(i,j; i,j+1)} = q_{(i,j; i,j+1)} C_{(i,j)} \quad (30)$$

where  $J_{c(i,j; i,j+1)}$  is the mass flow of the solute in cell (i,j) to cell (i,j+1).

Vertical mass flow

The mass flow of the solute in cell (i-1, j) to cell (i,j) and cell (i, j) to cell (i+1, j) is determined by:

$$J_{c(i-1,j; i,j)} = q_{(i-1,j; i,j)} C_{(i-1,j)} \quad (31)$$

$$J_{c(i,j; i+1,j)} = q_{(i,j; i+1,j)} C_{(i,j)} \quad (32)$$

Mass transport of solute between adjacent rings

The mass (M) of solute that passes from one ring to another (E) in both the horizontal and vertical direction, is calculated by the following mathematical relationships:

Radial direction

$$Ec_{(i,j-1; i,j)} = J_{c(i,j-1; i,j)} 2\pi R_{(i,j-1)} \Delta z \Delta t \quad (33)$$

where  $Ec_{(i,j-1; i,j)}$  is the mass of solute passing through the cell (i, j-1) to cell (i,j), M.

$$Ec_{(i,j; i,j+1)} = J_{c(i,j; i,j+1)} 2\pi R_{(i,j)} \Delta z \Delta t \quad (34)$$

where  $Ec_{(i,j; i,j+1)}$  is the mass of solute passing through the cell (i,j) to cell (i,j+1), M.

Vertical direction

$$Ec_{(i-1,j; i,j)} = J_{c(i-1,j; i,j)} \pi (R_{(i,j)}^2 - R_{(i,j-1)}^2) \Delta t \quad (35)$$

$$Ec_{(i,j; i+1,j)} = J_{c(i,j; i+1,j)} \pi (R_{(i,j)}^2 - R_{(i,j-1)}^2) \Delta t \quad (36)$$

### 2.3.2 Flow by hydrodynamic dispersion

Before the calculation of flow by hydrodynamic dispersion, we determined the parameters of the diffusion coefficient or molecular ion ( $D_m$ , with dimensions  $L^2T^{-1}$ ) and hydrodynamic dispersion coefficient ( $D$ , with dimensions  $L^2T^{-1}$ ) for each increment  $\Delta t$  between consecutive cells:

$$D = D_m + \left( \frac{\lambda q}{\theta} \right) \quad (37)$$

where  $\bar{\theta}$  is the the average humidity between rings or consecutive cells.

Then the flow equation of hydrodynamic dispersion of solutes in soil can be written as:

$$Jdh = -\bar{\theta} D \frac{\Delta C}{\Delta s} \quad (38)$$

where  $Jdh$  is the hydrodynamic dispersion flow ( $ML^{-2}T^{-1}$ ).

From equation (38) calculates the flow by hydrodynamic dispersion, both horizontally and vertically, with the number of equations 39 to 42:

Radial flow by hydrodynamic dispersion

$$Jdh_{(i,j-1;i,j)} = -\left(\frac{\theta_{(i,j-1)} + \theta_{(i,j)}}{2}\right) D_{(i,j-1;i,j)} \left[\frac{C_{(i,j)} - C_{(i,j-1)}}{\Delta r}\right] \quad (39)$$

$$Jdh_{(i,j;i,j+1)} = -\left(\frac{\theta_{(i,j)} + \theta_{(i,j+1)}}{2}\right) D_{(i,j;i,j+1)} \left[\frac{C_{(i,j+1)} - C_{(i,j)}}{\Delta r}\right] \quad (40)$$

Vertical flow by hydrodynamic dispersion

$$Jdh_{(i-1,j;i,j)} = -\left(\frac{\theta_{(i-1,j)} + \theta_{(i,j)}}{2}\right) D_{(i-1,j;i,j)} \left[\frac{C_{(i,j)} - C_{(i-1,j)}}{\Delta z}\right] \quad (41)$$

$$Jdh_{(i,j;i+1,j)} = -\left(\frac{\theta_{(i,j)} + \theta_{(i+1,j)}}{2}\right) D_{(i,j;i+1,j)} \left[\frac{C_{(i+1,j)} - C_{(i,j)}}{\Delta z}\right] \quad (42)$$

Solute transport by dispersion hydrodynamics between rings

Analogous to the convective motion of solutes was calculated solute mass ( $E$ ) which passes from one ring to another in the radial and vertical directions.

Radial direction

$$Edh_{(i,j-1;i,j)} = Jh_{(i,j-1;i,j)} 2\pi R_{(i,j-1)} \Delta z \Delta t \quad (43)$$

$$Edh_{(i,j;i,j+1)} = Jh_{(i,j;i,j+1)} 2\pi R_{(i,j)} \Delta z \Delta t \quad (44)$$

Vertical direction

$$Edh_{(i-1,j;i,j)} = Jh_{(i-1,j;i,j)} \pi (R_{(i,j)}^2 - R_{(i,j-1)}^2) \Delta t \quad (45)$$

$$Edh_{(i,j;i+1,j)} = Jh_{(i,j;i+1,j)} \pi (R_{(i,j)}^2 - R_{(i,j-1)}^2) \Delta t \quad (46)$$

### 2.3.3 Solute balance in each ring

Similarly to the case of transport of water after applying the solution by a point source, we calculated the concentration of solute in the ring located at the depth ( $i$ ) and horizontal ( $j$ ) for each increment of time ( $\Delta t$ ). The amount of solute that was remaining in a ring after the

increment  $\Delta t$  is represented by the change in solute mass in the ring ( $\Delta E_{(i,j)}$ ) due to mass gain by:

Convection ( $E_{cg}$ ):

$$E_{cg(i,j)} = E_{c(i,j-1; i,j)} + E_{c(i-1,j; i,j)} \quad (47)$$

Hydrodynamic dispersion ( $E_{hg}$ )

$$E_{hg(i,j)} = E_{h(i,j-1; i,j)} + E_{h(i-1,j; i,j)} \quad (48)$$

and mass loss by:

Convection ( $E_{cp}$ ):

$$E_{cp(i,j)} = E_{cp(i,j; i,j+1)} + E_{cp(i,j; i+1,j)} \quad (49)$$

Hydrodynamic dispersion ( $E_{hp}$ )

$$E_{hp(i,j)} = E_{hp(i,j; i,j+1)} + E_{hp(i,j; i+1,j)} \quad (50)$$

obtaining finally:

$$\Delta E_{(i,j)} = \frac{E_{cg(i,j)} + E_{hg(i,j)} - E_{cp(i,j)} - E_{hp(i,j)}}{Fr} \quad (51)$$

Consequently, the new concentration of solute in the ring at the end of  $\Delta t$  is determined by the following equation:

$$C_{(i,j)} = \left[ \frac{\frac{C_{(i,jini)}}{(\theta_{(i,jini)} V_{s(i,j)})^{-1}} + \Delta E_{(i,j)}}{\theta_{(i,j)} V_{s(i,j)}} \right] \quad (52)$$

where  $C_{(i,jini)}$  is the solute concentration at the beginning of the interval  $\Delta t$ ,  $ML^{-3}$ .

When applying the technique to control volume discretization, equation (2) to two dimensions can be rewritten as:

$$Fr \frac{\Delta \theta C}{\Delta t} = -\frac{\Delta(qC)}{\Delta z} + \frac{\Delta}{\Delta z} \left[ D \bar{\theta} \frac{\Delta C}{\Delta z} \right] - \frac{\Delta(qC)}{\Delta x} + \frac{\Delta}{\Delta x} \left[ D \bar{\theta} \frac{\Delta C}{\Delta x} \right] \quad (53)$$

### 3. Model validation

The soil used in the validation of the model was derived from a profile classified as Oxisol, sandy phase, called Series "Sertaozinho". Soil moisture was determined by gravimetric method to a depth of 100 cm. For sampling in layers of 10 cm was used cup hole coupled to a jacketed system using a PVC tube to prevent contamination of the lower layers.

#### 3.1 Breakthrough curve and the solute transport parameters

In the validation of the model was used potassium ion. With the aim of obtaining the transport parameters of potassium in the wet bulb from the breakthrough curve, was

Parameters of water retention curve				
$\theta_r$	$\theta_s$	$\alpha$	n	m
( $\text{cm}^3\text{cm}^{-3}$ )	( $\text{cm}^3\text{cm}^{-3}$ )	( $\text{cm}^{-1}$ )		
0,113	0,482	0,029428	1,828069	0,452975

Table 1. Parameters of water retention, according to the model (van Genuchten 1980)

mounted an experiment which was used as solute potassium chloride, with a potassium concentration of 500 mgL<sup>-1</sup>. The values of potassium concentration, pore volume and cumulative time were used as input data CXTFIT program developed by U.S. Salinity Laboratory, USDA, Riverside, CA, version 2.1, written in FORTRAN. The CXTFIT determines the values of the parameters of solute transport in soil that is the dispersion coefficient (D), the pore water velocity (V), the dispersivity ( $\lambda$ ) and retardation factor (Fr), through attempts to maximize the coefficient of determination of regression between the averaged concentration on the solution (C/Co) and pore volume. Thus, we obtained the values of transport parameters that are shown in Figure 3 (breakthrough curve) and Table 2

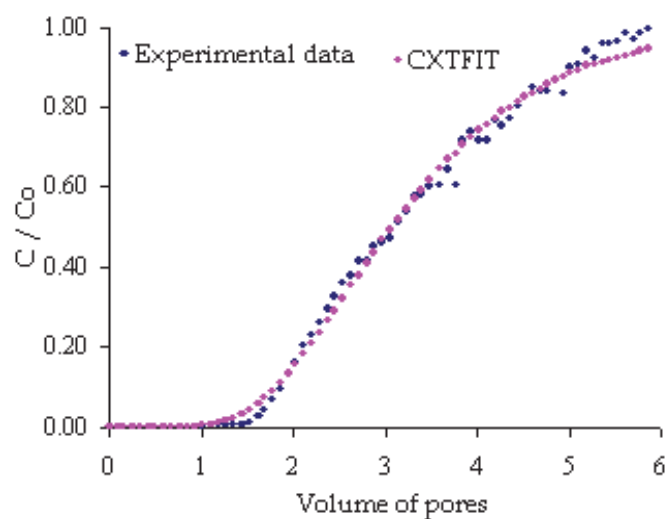


Fig. 3. Breakthrough curve of potassium solution in the soil column.

Transport parameters of potassium			
V	D	Fr	$\lambda$
( $\text{cm min}^{-1}$ )	( $\text{cm}^2 \text{min}^{-1}$ )	(adimensional)	(cm)
1,489	2,705	4,730	1,816655

Table 2. Transport parameters of potassium in the soil obtained from the model CXTFIT: pore water velocity (V), dispersion-diffusion coefficient (D), retardation factor (Fr) and dispersivity ( $\lambda$ )

3.2 Soil moisture after irrigation

Data of soil moisture after 24 hours after irrigation generated by the model and the observed are presented through moisture isolines in Figure 4. Inside the bulb, ie a radius of 26 cm and depth of 30 cm from the emitter soil moisture varies in a range from 0.17 to 0.20 cm<sup>3</sup> cm<sup>-3</sup>,

decreasing both in the radial or vertical direction, as it away from the emitter, the bulb acquiring a hemispherical shape. Observe that the radius of the bulb was slightly greater than its depth. In this respect Hachum et al. (1976) indicate that the force of gravity has a limited effect on clay and loam soils and, where capillary forces dominate the effects on water flow.

Outside the region of the bulb, there was practically no change in moisture content, which allowed the sampling was done only up to a radius of 50 cm and 70 cm deep, including therefore a safety margin.

The water content in the center of concentric rings (where it was located the point source) was approximately  $0.20 \text{ cm}^3 \text{ cm}^{-3}$  in both cases (observed and simulated). This represents a little less than half the moisture saturation ( $0.43 \text{ cm}^3 \text{ cm}^{-3}$ ), indicating that the time interval elapsed since the completion of irrigation until the moment of sampling (24 hours) there was a marked redistribution of the solution.

The soil moisture obtained (simulated and observed) were similar, being a value for the standard error of  $0.011 \text{ cm}^3 \text{ cm}^{-3}$ . The central axis, the wet bulb has reached 35 cm with a moisture content of  $0.176$  and  $0.172 \text{ cm}^3 \text{ cm}^{-3}$  for the model and test, respectively. As for the periphery (at 35 cm radius) the bulb has reached 20 cm depth for the model and about 15 cm depth for the test with moisture content of  $0.170$  and  $0.163 \text{ cm}^3 \text{ cm}^{-3}$ , respectively.

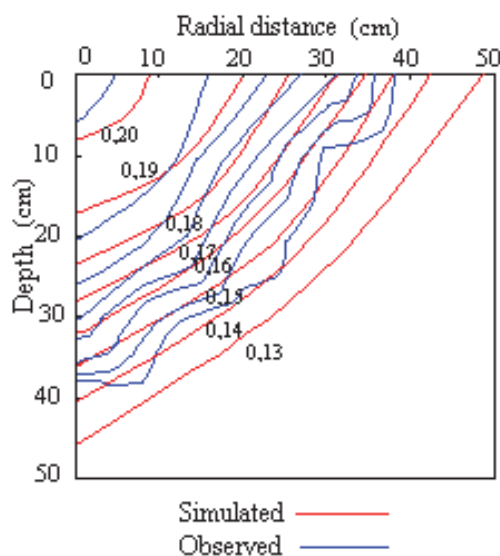


Fig. 4. Volumetric soil water content ( $\text{cm}^3 \text{ cm}^{-3}$ ) simulated by the model and observed 24 hours after the end of irrigation.

For a time of redistribution of 48 hours after irrigation, the dimensions of the bulb remained constant when compared with the time of 24 hours of redistribution, but there was a decrease in humidity, especially in cells near the point source. On the ground surface, a radial distance of 10 cm, volumetric soil water content was approximately  $0.18 \text{ cm}^3 \text{ cm}^{-3}$  for the two cases (simulated and observed), suffering a decrease of approximately 7.5% moisture when compared with a time of 24 hours. The simulated moisture values were slightly higher than those observed, but the trend of the data in different cells was the same, determining a value for the standard error of  $0.015 \text{ cm}^3 \text{ cm}^{-3}$ .

Elapsed time of 72 hours after irrigation, in both conditions (simulated and observed) cells close to the point source continued losing water to the adjacent cells, leaving a soil moisture

around the  $0.178 \text{ cm}^3 \text{ cm}^{-3}$ , which represents a decrease of 5% over the 48 hours time, but still, this did not contribute significantly to changes in the dimensions of the bulb. Both humidity (simulated and observed) had an approximate behavior with regard to the distribution of moisture, resulting in a value for the standard error of  $0.008 \text{ cm}^3 \text{ cm}^{-3}$ . In this type of soil, one can say that 24 hours after the redistribution of water within the wetted practically ends with the largest changes observed in cells near the sender, ie the water flow that occurred after this time was small, so that the bulb dimensions have to remain virtually unchanged.

In general, the experimental values were similar to the model simulated. Small differences should possibly be due to limitations of the model and accuracy of measurements. It is important to emphasize that the assumptions made in developing the model were that the soil is homogeneous, there is no evaporation, the initial water content in soil is uniform, there is no occurrence of hysteresis, and the water applied by the issuer is distributed uniformly in all directions. Moreover, the model assumed average values for hydraulic conductivity between two adjacent cells, whereas in reality the change from one point to another is gradual. Already Nogueira et al. (2000) used the harmonic mean of three layers in the determination of hydraulic conductivity. In relation to homogeneous and isotropic soil, there was possibly a variation of physical and hydraulic properties in soil, thus filling the box with soil was done in layers of 10 cm, a fact that probably involves a change in soil density. With respect to evaporation during the test there was a slight condensation of water at the bottom of the plastic covering the box. Regarding the hysteresis, according to Levin et al. (1979), during the redistribution due to the low levels of soil moisture on the periphery of the bulb, the hysteresis has a pronounced influence, which may have occurred in the test.

Another fact during testing is the formation of a thin crust under the emitter, possibly by the dispersion of particles during application of the solution, which probably led to a reduction in porosity and hydraulic conductivity in this region, which was also observed by Lafolie et al. (1989). Also do not rule out a possible contamination of soil layers has been made when sampling with the auger, but has since been made the hole when the jacketing of sampling, there may have been the contact of small amounts of soil.

### 3.3 Concentration of potassium in the soil after irrigation

Potassium is adsorbed by clay particles, this fact can be seen in Table 2, reveals that to obtain a value for the retardation factor ( $Fr$ ) equal to 4.73 (similar to that found by Miranda (2001) for the same soil type) indicating that one part of potassium applied to the solution is retained by the soil.

The results obtained in the concentration of potassium in the soil solution in different cells 24 hours after irrigation for both simulated and observed, are shown in Figure 5. This cation was retained in the surface layers. For both simulated and observed highest concentrations were around the emitter in a radius of 10 cm and 20 cm depth, where concentrations of potassium ranged from 62 to  $817 \text{ mg L}^{-1}$ .

The volume of soil containing considerable amounts of potassium (potash bulb) was lower than the wet bulb. The displacement of this cation is not fully followed the displacement of water (mass or convective flow). This can be explained by potassium in the soil solution interact with the cationic exchange complex of soil (expressed by the retardation factor), and therefore this element retained in the soil in the region closer to the emitter, so that the solution that went into the outer regions of the bulb possibly possessed a lower concentration of potassium. The values of potassium concentration simulated by the model



were similar to those observed in the test (with a value for the standard error of  $30.07 \text{ mg L}^{-1}$ ), following the same pattern of distribution. However, in general, the experimental values were slightly lower than those generated by the model.

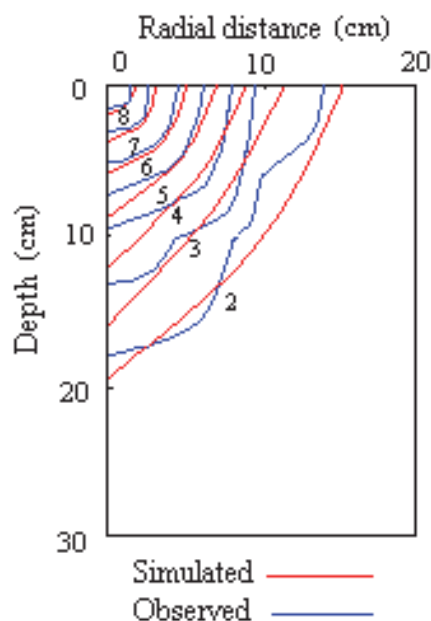


Fig. 5. Potassium concentration in soil solution ( $\text{mg L}^{-1} \times 100$ ) simulated and observed 24 hours after irrigation.

For a time of redistribution of 48 hours after irrigation the content of potassium in the bulb cells remained in an almost unchanged, although the concentration of this element in general have risen as a result of decreased water content in the cells. The potassium present in soil solution in the rings located between 10 and 20 cm shaft showed concentrations ranging from 46 to  $250 \text{ mg L}^{-1}$  for both cases, showed similar trend and, with a standard error equal to  $12.67 \text{ mg L}^{-1}$  (in this case for less than 24 hours), the difference between simulated and observed values was in the range of 10%.

The content of potassium into cells in the soil 72 hours after irrigation has remained virtually unchanged with respect to that shown for 48 hours, and the concentration of this element on the soil surface within a radius of 10 to 20 cm from the emitter, ranged between 48 and  $258 \text{ mg L}^{-1}$ , with differences between predicted and observed roughly 12% with a value for the standard error of  $11.30 \text{ mg L}^{-1}$ , slightly lower than the value obtained for 48 hours.

Overall, the three times of redistribution considered, the concentration of potassium in the soil solution simulated by the model was similar to that seen in experimental conditions, and the displacement of this element partially followed the displacement of water, focusing primarily on cells more internal bulb. As explained in the case of moisture, the differences found between the concentrations of potassium possibly simulated and observed were mainly due to limitations of the model, because during development were not considered the process of hysteresis, considering only movement and adsorption process. Also soil physical-hydric variation, the errors in sampling and errors in determining the averaged concentration of potassium in solution in the laboratory.

It was also observed for the three times of redistribution, the values of potassium concentration obtained experimentally were lower than those generated by the model,



which may be due to variations in bulk density in filling the box soil, the interaction of potassium soil solution with the other cations in the exchange complex of soil, as Ca, Na, Mg and Al. In addition the fact that the determination of the retardation factor was made in a soil washed with distilled water under conditions saturation practically free of cations in solution, which might not exactly represent the delay of potassium that occurs under real conditions, when cells of the bulb are under different levels of moisture (unsaturated condition) and when there are other cations in soil solution.

Moreover, the concentration of potassium observed in the three study time showed very low rates of redistribution and concentrated on the soil surface in the vicinity of emitter, which shows that besides being trapped in the inner layers to interact with the soil matrix, potassium is transported mainly by convective flow with the water (also called mass flow) in proportion to its flow and concentration. Therefore, the general pattern of distribution of potassium in the soil considered by the model, is dependent on the initial concentration of soil solution, the concentration in irrigation water, the emitter flow and physical-chemical properties of soil.

**3.4 Sensitivity analysis of the moisture distribution in the bulb**

As seen in Figure 6 respect to the saturated hydraulic conductivity, it appears that this has a important effect on the moisture of the bulb, especially when varied negatively, however for positive increments of the a standard error curve had lower slopes, and the model therefore less sensitive to increases in hydraulic conductivity than the reductions in this parameter.

The moisture content of the bulb is very sensitive to moisture changes of soil saturation, however, when this parameter begins to decrease (due to a reduction in porosity), the cells become saturated near the emitter, and begins to form a water depth at the soil surface, an aspect that is no longer considered by the model.

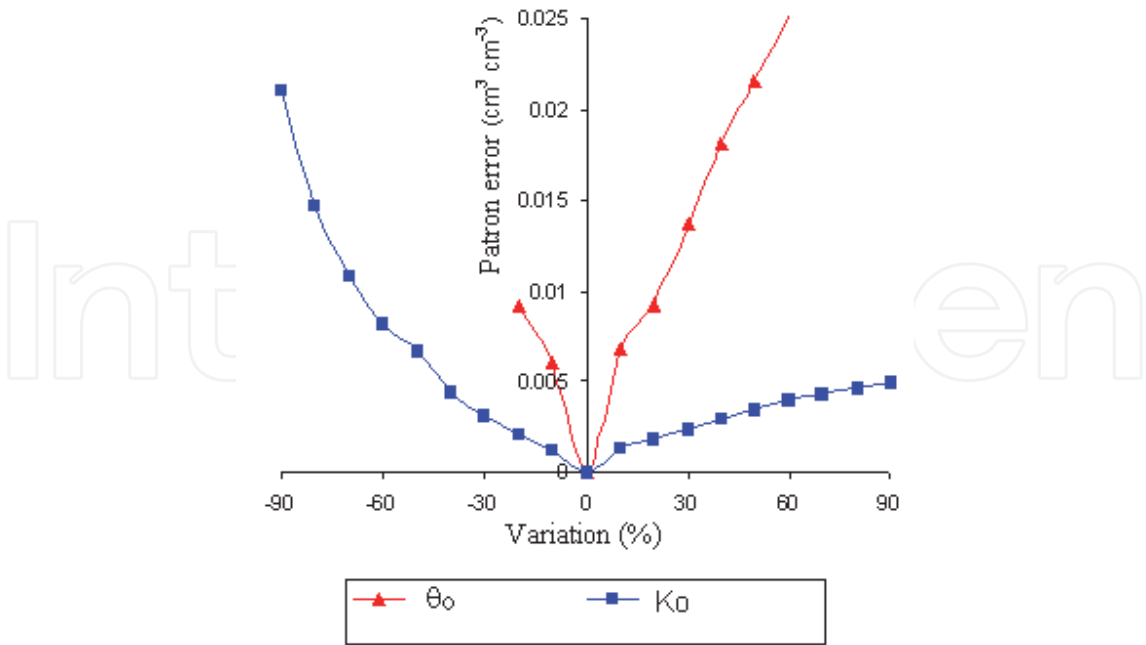


Fig. 6. Representation of the sensitivity analysis of the model with the profile of soil moisture on the bulb, applying from -90% to + 90% variation in soil moisture saturation ( $\theta_0$ ) and saturated hydraulic conductivity ( $K_0$ ).

### 3.5 Sensitivity analysis of the potassium distribution in the bulb

As can be seen in Figure 7 referred to the saturated hydraulic conductivity, the model is sensitive to this parameter decreases, especially for very low values. For positive changes, the model is little sensitive, and be almost insensitive to high values of  $K_0$ .

With regard to soil moisture at saturation, the model is sensitivity to small increments of  $\theta_0$ . For decreases of  $\theta_0$  behavior is similar, but to a limited extent, as the soil begins to soak causing the impossibilities already discussed. The sensitivity of the model on this parameter was lower than that in the case of distribution of moisture in the bulb, because the potassium does not follow exactly the same dynamics of soil water.

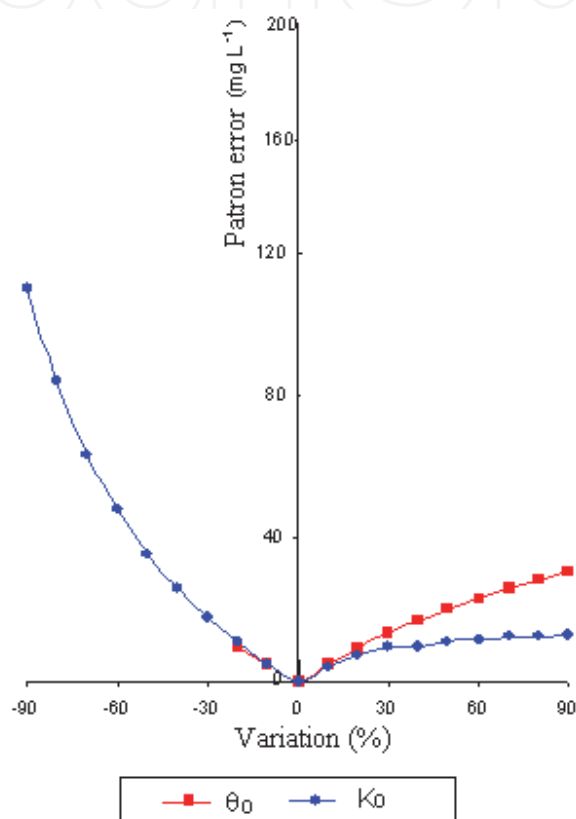


Fig. 7. Representation of the sensitivity analysis of the model relative to the concentration of potassium in the bulb, applying from -90% to + 90% variation in soil moisture saturation ( $\theta_0$ ) and saturated hydraulic conductivity ( $K_0$ ).

## 4. Conclusions

The movement and distribution of water and potassium applied through drip irrigation can be modeled mathematically by the solution of the equations of transient flow by using the method of control volumes. There was a good fit in the values of the distribution of water and potassium in the bulb when compared to data simulated by the model with experimental data, yielding average values for the standard error equal to 0.0114 cm<sup>3</sup> cm<sup>-3</sup> and 18.013 mg L<sup>-1</sup> to moisture and potassium, respectively. The potassium distribution was limited to the inner layers of the bulb, which delayed the shift of this cation to interact with the soil matrix. The model, with respect to the distribution of soil water, is very sensitive to moisture saturation variations and moderately sensitive to hydraulic conductivity for

saturated soil, on the other hand potassium distribution is affected mainly by the physical-chemical soil properties, therefore the model is very sensitive to negative variations of hydraulic conductivity for saturated soil.

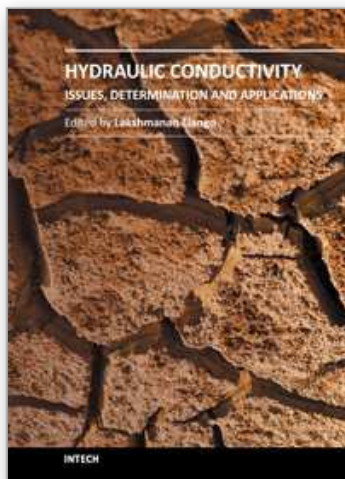
## 5. References

- Alvarez, J.; Herguedas, A; Atienza, J. (1995). *Modelización numerica y estimación de parámetros para la descripción del transporte de solutos en columnas de suelo en laboratorio*. Madrid: INIA. 69p.
- Botrel, T. A. (1988). *Simulação da distribuição espacial da água em solo irrigado com gotejador*. Piracicaba. 61p. Tese (Doutorado) - Escola Superior de Agricultura "Luiz de Queiroz", Universidade de São Paulo.
- Cruz, R. L. (2000). *Modelização do balanço hídrico de uma cultura irrigada por um sistema de irrigação localizada*. Botucatu. 80 p. Tese (Livre Docente) - Faculdade de Ciências Agronômicas, Universidade Estadual Paulista "Júlio de Mesquita Filho".
- Hachum, A. Y.; Alfaro, J. F.; Willardson, L. S. (1976). Water movement in soil from trickle source. *Journal of Irrigation and Drainage Engineering*, v.102, n.2, p.179-192.
- Lafolie, F.; Guennelon, R.; van Genuchten, M. Th. (1989). Analysis of water flow under trickle irrigation: I Theory and numerical solution. *Soil Science Society American Journal*, n. 53, p. 1310-1318.
- Levin, I.; van Rooyen, P. C.; van Rooyen, F. C. (1979). The effect of discharge rate and intermitent water application by point-source irrigation on the soil moisture distribution pattern. *Soil Science Society American Journal*, n. 43, p. 8-16.
- Matos, A. T.; Costa, L. M.; Fontes, M. P.; Martinez, M. A. (1999). Retardation factors and the dispersion-diffusion coefficients of Zn, Cd, Cu and Pb in soils from Viçosa-MG, Brazil. *Transactions of the ASAE*, v. 42, n.4, p.903-910.
- Miranda, J. H. (2001). *Modelo para simulação da dinâmica de nitrato em colunas verticais de solo não saturado*. Piracicaba. 79 p. Tese (Doutorado) - Escola Superior de Agricultura "Luiz de Queiroz", Universidade de São Paulo.
- Mualem, Y. A. (1976). A new model for predicting the hidraulic conductivity of unsaturated porous media. *Water Resources Research*, v. 12, n.3, p.513-522.
- Nielsen, D. R.; Biggar, J. W. (1962). Miscible displacement: III. Theoretical considerations. *Soil Science Society of American Proceedings*, v. 26, n. 2, p.216-221.
- Nogueira, C. P.; Coelho, E. F.; Leão M. C. S. (2000). Características e dimensões do volume de um solo molhado sob gotejamento superficial e subsuperficial. *Revista Brasileira de Engenharia Agrícola e Ambiental*, v. 4, n. 3, p.315-320.
- Toride, N.; Leij, F. van Genuchten, M. Th. (1999). *The CXTFIT code for estimating parameters from laboratory or field tracer experiments, verion 2.1*. Califórnia: Research Report U. S.; Salinity Laboratory Agricultural Research Service; U. S. Departament of Agriculture. 85p.
- van Der Ploeg, R. R.; Benecke, P. (1974). Unsteady unsaturated, n-dimensional moisture flow in soil: a computer simulation program. *Soil Science Society of America Proceedings*, v.38, p. 881-885.

- van Genuchten, M. Th. (1980). A closed form equation for predicting the hydraulic conductivity of unsaturated Soils. *Soil Science Society American Journal*, v. 44, p. 892-898.
- van Genuchten, M. Th.; Wierenga, P. J. (1986). Solute dispersion coefficients and retardation factors. In: KLUTE, A. *Methods of Soil Analysis. I-Physical and Mineralogical Methods*. Madison: Soil Science Society of America. p.1025-1054.

IntechOpen

IntechOpen



## **Hydraulic Conductivity - Issues, Determination and Applications**

Edited by Prof. Lakshmanan Elango

ISBN 978-953-307-288-3

Hard cover, 434 pages

**Publisher** InTech

**Published online** 23, November, 2011

**Published in print edition** November, 2011

There are several books on broad aspects of hydrogeology, groundwater hydrology and geohydrology, which do not discuss in detail on the intrigues of hydraulic conductivity elaborately. However, this book on Hydraulic Conductivity presents comprehensive reviews of new measurements and numerical techniques for estimating hydraulic conductivity. This is achieved by the chapters written by various experts in this field of research into a number of clustered themes covering different aspects of hydraulic conductivity. The sections in the book are: Hydraulic conductivity and its importance, Hydraulic conductivity and plant systems, Determination by mathematical and laboratory methods, Determination by field techniques and Modelling and hydraulic conductivity. Each of these sections of the book includes chapters highlighting the salient aspects and most of these chapters explain the facts with the help of some case studies. Thus this book has a good mix of chapters dealing with various and vital aspects of hydraulic conductivity from various authors of different countries.

### **How to reference**

In order to correctly reference this scholarly work, feel free to copy and paste the following:

René Chipana Rivera (2011). The Role of Hydraulic Conductivity in Modeling the Movement of Water and Solutes in Soil Under Drip Irrigation, Hydraulic Conductivity - Issues, Determination and Applications, Prof. Lakshmanan Elango (Ed.), ISBN: 978-953-307-288-3, InTech, Available from:  
<http://www.intechopen.com/books/hydraulic-conductivity-issues-determination-and-applications/the-role-of-hydraulic-conductivity-in-modeling-the-movement-of-water-and-solutes-in-soil-under-drip->

**INTECH**  
open science | open minds

### **InTech Europe**

University Campus STeP Ri  
Slavka Krautzeka 83/A  
51000 Rijeka, Croatia  
Phone: +385 (51) 770 447  
Fax: +385 (51) 686 166  
[www.intechopen.com](http://www.intechopen.com)

### **InTech China**

Unit 405, Office Block, Hotel Equatorial Shanghai  
No.65, Yan An Road (West), Shanghai, 200040, China  
中国上海市延安西路65号上海国际贵都大饭店办公楼405单元  
Phone: +86-21-62489820  
Fax: +86-21-62489821

© 2011 The Author(s). Licensee IntechOpen. This is an open access article distributed under the terms of the [Creative Commons Attribution 3.0 License](https://creativecommons.org/licenses/by/3.0/), which permits unrestricted use, distribution, and reproduction in any medium, provided the original work is properly cited.

IntechOpen

IntechOpen